

SURFACE STABILITY OF EPITAXIAL $\text{LaNiO}_{3-\delta}$ THIN FILMS

S. Mickevičius^a, S. Grebinskij^a, V. Bondarenka^{a,b}, H. Tvardauskas^a, M. Senulis^a,
V. LISAUSKAS^a, K. Šliužienė^a, B. Vengalis^a, B.A. Orłowski^c, and E. Baškys^a

^a *Semiconductor Physics Institute, Center for Physical Sciences and Technology, A. Goštauto 11, LT-01108 Vilnius, Lithuania*
E-mail: sigism@pfi.lt

^b *Vilnius Pedagogical University, Studentų 39, LT-08106 Vilnius, Lithuania*

^c *Institute of Physics of the Polish Academy of Sciences, Al. Lotników 32/46, 02-668 Warsaw, Poland*

Received 3 December 2009; revised 23 June 2010; accepted 16 September 2010

Thin $\text{LaNiO}_{3-\delta}$ films with pseudocubic (100) preferred orientation were prepared by reactive DC magnetron sputtering and *in situ* annealed in O_2 and vacuum. X-ray photoelectron spectroscopy (XPS) was used to determine the variation in composition of the films under high temperature annealing. The experimental O 1s and La 3d – Ni 2p_{3/2} spectra of $\text{LaNiO}_{3-\delta}$ films was analysed in terms of O^{2-} , $\text{O}^-/(\text{OH})^-$, and weakly adsorbed oxygen species. It was shown that the change in the type of conductivity from metallic to semiconducting one is accompanied by a marked increase in the intensity of the lateral (~ 531 eV) peak of oxygen. The quantitative analyses of La 3d – Ni 2p_{3/2} spectra show that the Ni/La concentration ratio significantly decreases after heating above the dehydration temperature. These variations in conductivity and surface composition were attributed to the loss of lattice oxygen with subsequent adsorption of O^- and $(\text{OH})^-$ anions and weakly adsorbed oxygen species from ambient air.

Keywords: rare earth alloys and compounds, oxide materials, XPS, surfaces and interfaces, LaNiO_3 thin film

PACS: 68.60.Dv, 79.60.Dp

1. Introduction

In recent years, an increasing interest has been focused on metal oxides of oxygen octahedral structure due to their metal–insulator transition, high-temperature superconductivity, ferroelectricity, colossal magnetoresistance and on their heterostructures for future technological application potentials [1–4]. LaNiO_3 (LNO) is one of the few conductive oxides with a crystal structure suitable for integration in epitaxial heterostructures with perovskites because of its good transport properties, composition simplicity, and pseudocubic perovskite crystal structure with a lattice parameter $a = 3.84$ Å. In most studies, LNO films are considered as having good physical and chemical thermostabilities, and most metal oxide films, such as ferroelectric films, must be grown at a high temperature. Therefore, it is necessary to study the thermostability of these films.

It is known that considerable segregation of elements takes place in chemically synthesized $\text{LaNiO}_{3-\delta}$ samples, i. e. the surface concentration of various species differs from the volume one [5]. Another factor to be considered is the tendency of rare earth and nickel

oxides to absorb water vapour and carbon dioxide from air, so that any *ex situ* exposure of these films to air will result in an uncontrolled reaction and stoichiometry [6].

Lanthanum hydroxide, in turn, tends to adsorb humidity at the surface and to react with carbon dioxide from the atmosphere in order to form lanthanum carbonate.

A study on the thermostability of LaNiO_3 films prepared by RF magnetron sputtering and *in situ* annealed at 265 °C were performed [7]. It was demonstrated that electric and optical properties of LNO films are unstable even at a relatively low temperature. But the annealing does not affect the lattice structure. The electronic structure of high-quality LNO thin films was investigated *in situ* using photoemission spectroscopy [8]. In that work it was shown that O 1s X-ray absorption spectrum is in good agreement with previous studies on polycrystalline LNO surfaces.

It was shown earlier that epitaxial $\text{LaNiO}_{3-\delta}$ films deposited onto (100)-plane oriented NdGdO_3 substrate demonstrated excellent in-plane orientation [9] and the surface La/Ni ratio was close to the stoichiometric one [10].

Angle dependent spectra, obtained with the Tunable High-Energy X-ray Photoelectron Spectrometer at the X-ray wiggler beam line BW2 of HASYLAB (Hamburg) reveal that significant variations of oxide versus hydroxide concentrations occur within the thin surface layer even after long-term (one year) exposure to the atmosphere. Estimated thickness of this hydroxide enriched layer is of about 2 nm [11].

In this paper, LNO films are deposited on NdGaO₃ substrates by a reactive DC magnetron sputtering system, and their composition and electrical conductivity dependence on high temperature annealing have been investigated.

2. Experimental details

Thin LaNiO_{3-δ} films were deposited onto monocrystalline (100)-plane oriented NdGaO₃ substrate by using a reactive DC magnetron sputtering technique. The ceramical LaNiO₃ target (25 mm in diameter and 2.5 mm thick) was prepared by pressing at $5 \cdot 10^8$ Pa and after sintering in air at 1000 °C for 10 h the La₂O₃ and NiO (99.99% purity from Aldrich-Chemie) powders in the stoichiometric ratio. The sputtering was performed in Ar and O₂ mixture (20:1) at pressure of about 15 Pa. To prevent the film bombardment by high energy ions during deposition, NdGaO₃ substrates were positioned in “off-axis” configuration at a distance of 15 mm from the symmetry axis of the discharge and 20 mm over the target plane. The substrate temperature was ~ 750 °C. Under these conditions, the deposition rate was 25 nm/h, and the resultant thickness of LaNiO_{3-δ} film was about 0.1 μm. Films were annealed *in situ* in vacuum (10^{-5} Pa) or in O₂ atmosphere (10^5 Pa).

X-ray photoelectron spectra were recorded using XSAM 800 (KRATOS Analytical, UK). The photoelectrons were excited using a non-monochromatized Al K_α (1486.6 eV) radiation source at 15 kV, 300 W. We were forced to use this relatively wide excitation to avoid interference from overlapping Ni(L₃M₂₃M₂₃) Auger features with XPS O 1s region using a Mg K_α source. The analyzer was used in a fixed retarding ratio mode with an energy resolution $\Delta E/E = 0.08\%$. The working pressure in the analysis chamber was maintained below 10^{-7} Pa during the spectrum analysis.

Photoemission data were collected and processed by the KRATOS DS800 data system. After Al K_α satellites and background subtraction, the complex photoelectron spectra were decomposed into separate peaks by specifying the peak position – binding energy (BE),

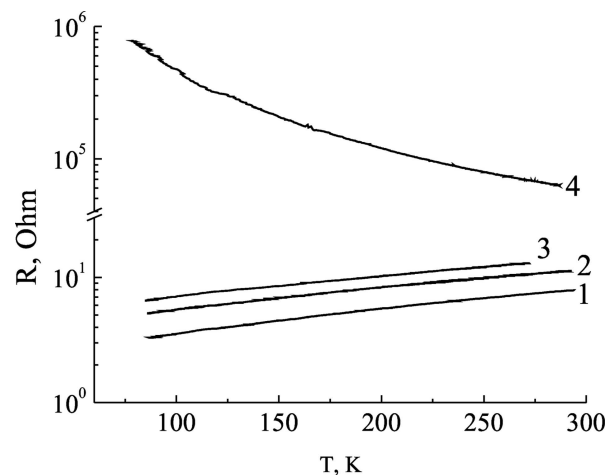


Fig. 1. Temperature dependence of LNO films resistance for as-grown film (curve 1), annealed in oxygen at 750 °C (curve 2), and in vacuum at 450 and 700 °C (curves 3 and 4 respectively).

area, width, and Gaussian/Lorentzian ratio. Because any mathematical operation (such as data smoothing) on the raw data would distort the original physical picture, no such treatment was permitted in the quantitative data analysis. The accuracy of the measured lines BE and relative intensities were about 0.1 eV and 10% respectively. To control the sample contamination, the survey spectra of an air-exposed, fresh sample have been studied. Only lanthanum, nickel, oxygen, and carbon lines were identified within the probing depth of XPS. No more contamination related to the sample preparation was detected by XPS within the accuracy of our measurements. The adventitious carbon C 1s line was used for the fine correction of charging effects, supposing its BE is equal to 284.6 eV.

The influence of ion sputtering on the chemical composition of investigated compounds was treated by using Ar⁺ ion bombardment at 2 keV and current density of $2 \mu\text{A cm}^{-2}$ during 1 min.

The electrical conductivity measurements were performed by a standard DC four-probe method in the 78–300 K temperature range.

3. Results and discussion

According to the temperature dependence of resistance shown in Fig. 1, films may be divided into two groups with a metallic and semiconducting type of conductivity (see Table 1). Drastic changes in O 1s XPS spectra (Fig. 2) after high (above 700 °C) temperature annealing indicate strongly that the heat treatment induced changes in the films composition are responsible for the conversion of the conductivity.

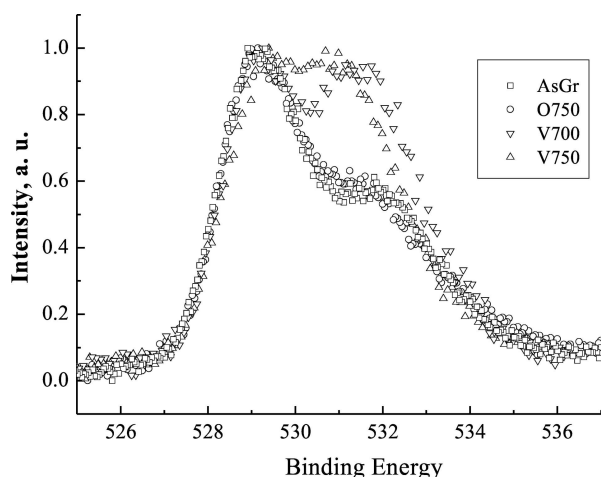


Fig. 2. O 1s comparison spectra for the LNO films with metallic (as-grown and O750) and semiconducting (V700 and V750) type of conductivity. Annealing conditions are listed in Table 1.

Table 1. Annealing conditions and conductivity type of studied films.

Film	Annealing condition		Conductivity type
	Temperature, °C	Atmosphere	
as-grown	—	—	metallic
O750	750	O ₂	metallic
V450	450	vacuum	metallic
V700	700	vacuum	semiconducting
V750	750	vacuum	semiconducting

O 1s spectra are rather complex and may be roughly separated into three regions.

In all cases, an intense peak is observed at low energy around 529 eV. This peak seems to be very similar for all samples and may be attributed to O²⁻ anions of the crystalline network.

Beside this peak, a second component can be observed at higher energies. Its intensity is strongly affected by the heat treatment. For metallic films, this component only slightly varies in intensity and always appears as a shoulder around 531 eV and drastically increases for samples with dielectric conductivity.

These lateral structures have been reported in many studies, but are not precisely attributed. The assumption of different valence states for the metal [12] or several final states [13] has been made, but in most cases this structure has been assigned to contamination surface species. The adsorption of (OH)⁻ or CO₃²⁻ groups was suggested in comparison with the binding energy of the O 1s peak in hydroxide or carbonate compounds; other adsorbed species such as O₂²⁻ were also proposed.

Jimenez et al. [14] attribute the lateral peak to low

coordinated oxygen ions at the surface of the samples. It was also suggested [15] that the oxygen partial integration might occur in the bulk and generate a high binding energy component, more or less intense, for the O 1s peak. In a mixed oxygen chemisorption-penetration situation, bond lengths and crystal potentials may vary significantly leading to a range of O 1s binding energies; this may also account for the large width and variable BE positions of the lateral structure. Moreover, (OH)⁻ in LNO may be in two forms: hydro- and oxyhydroxides [16] with a close, but different O 1s core level BE in lateral peak energies range.

The high energy tail may include physisorbed (~534 eV), chemisorbed (~532 eV), structural H₂O and water in poor electrical contact with the films surface [17, 18]. In general, it may be concluded that numerous oxygen species with a BE distributed within a wide energy range may be involved in final O 1s spectra of LNO surface [19].

It is evident that these various oxygen contributions cannot be fitted in an unambiguous way even for XPS spectra obtained without considerable noise and with good resolution.

To obtain meaningful information about the surface composition from fitting results, one needs additional knowledge about the corresponding peaks nature and position. Such *a priori* information is highly desirable for the correct selection of an initial approximation in fitting experimental data, since the existence of local minima may lead to erroneous results.

Additional thermal treatments and ionic etching were realized in order to clarify the nature of species, contributing to O 1s spectra in the intermediate energy range. A highly resistive ($R > 10 \text{ M}\Omega$) film V750 with a semiconducting type of temperature behaviour was selected for this purpose. An *in situ* bombardment with Ar⁺ ions of 2 keV energy for 1 min was used for the surface cleaning.

After the deposition, the film was exposed to air for several days. Then it was placed in a vacuum chamber and XPS measurements were done for as-grown and Ar⁺ etched samples. Then the temperature was raised up to 550 °C and after a 30 hour exposure the XPS spectra were measured at this temperature and after slow (~100 °C/h) cooling down to room temperature. Finally, the film was exposed to air for 2 hours with a subsequent XPS analysis. The results are presented in Fig. 3. Note that spectra measured at 550 °C and after cooling were absolutely identical.

It is evident from the comparison spectra (Fig. 3, curves 1 and 2) that weakly absorbed species can be

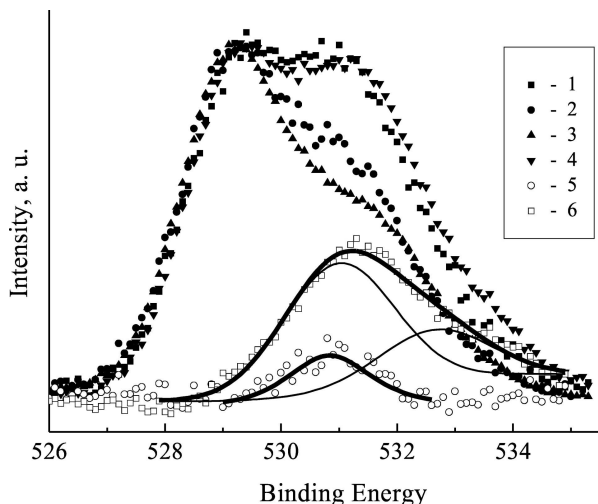


Fig. 3. Comparison (filled symbols) and difference (open symbols) spectra of highly-resistive dielectric LNO film V750 before any treatment (1) and after subsequent: Ar^+ polishing (2), super high vacuum annealing (550°C ; 30 h) (3), and exposure to ambient air for 2 hours (4). Curves 5 and 6 represent the difference of 2–3 and 4–3 spectra respectively. Symbols correspond to experimental data, the thick solid line to the fitted difference spectra envelope, and thin lines to spectral components of difference spectra.

effectively removed by low-intensity Ar^+ polishing. Further annealing leads to an additional decrease in the lateral peak (~ 531 eV) intensity and may be related to the film dehydration. It is known that thermal transformation from lanthanum hydroxide to oxide is a two-step mechanism [16, 20]. The intermediate product is lanthanum hydroxide oxide: $\text{La}(\text{OH})_3 \rightarrow \text{LaOOH} + \text{H}_2\text{O}$ ($310\text{--}340^\circ\text{C}$). Lanthanum hydroxide oxide decomposes in a second step in order to form the oxide according to $2\text{LaOOH} \rightarrow \text{La}_2\text{O}_3 + \text{H}_2\text{O}$ ($450\text{--}500^\circ\text{C}$).

Thus, the single-peak difference spectra (Fig. 3, curve 5) may be attributed to hydroxide and/or oxyhydroxide at BE of about 531 eV and one would expect the full dehydration of LNO films. Then the shoulder (~ 531 eV) on the O 1s spectra may be attributed to tightly bonded oxygen species, probably surface and/or low coordinated oxygen. Unfortunately, the maximum available annealing temperature (550°C) is not sufficient for the thermal decomposition of carbonate species: $\text{La}_2\text{O}_2\text{CO}_3 \rightarrow \text{La}_2\text{O}_3 + \text{CO}_2$ ($600\text{--}800^\circ\text{C}$) and possible surface contamination with these species cannot be excluded.

The XPS spectra of La 3d and Ni $2p_{3/2}$ spectra region before and after film annealing at high temperature are presented in Fig. 4. Lanthanum oxide/hydroxide ratio was estimated from the relative areas of peaks corresponding to the oxide and hydroxide species, obtained from La $3d_{5/2}$ spectra fitting. This ratio was 0.3 and 1.4 for as-grown and annealed sample, re-

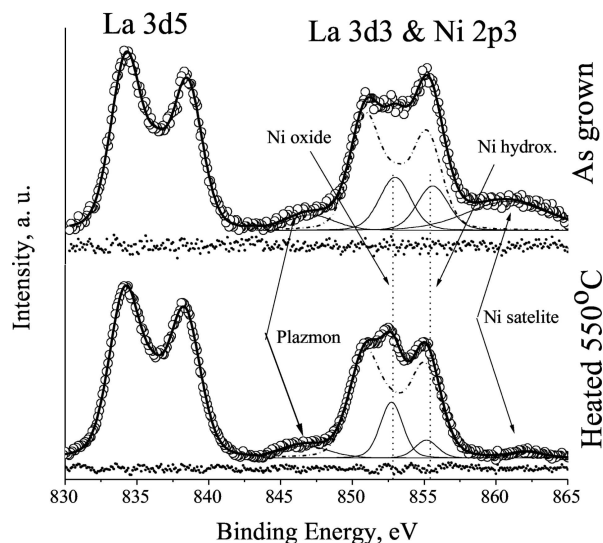


Fig. 4. La 3d and Ni $2p_{3/2}$ spectra of $\text{LaNiO}_{3-\delta}$ thin film (exposed to laboratory ambient conditions for one day) measured before and after heat treatment. Symbols are matches to the experimental data, the thick solid line to the fitted spectra envelope, dashed line to the La $3d_{3/2}$ spectra envelope, and thin lines to spectral components. Points correspond to residual spectrum.

spectively. These results indicate that after annealing the lanthanum oxide/hydroxide ratio significantly increases.

The significant variations in the La $3d_{3/2}$ – Ni $2p_{3/2}$ spectra region after the heating above dehydration temperature (Fig. 4) may be attributed to the partial disappearance of the nickel species as a result of the nickel hydroxide evaporation/decomposition at temperatures exceeding the melting point $T_m = 230^\circ\text{C}$ [21]. The significant decrease of nickel/lanthanum concentration ratio from $\text{Ni}/\text{La} = 1.02$ (close to stoichiometric one) for the as-grown sample to $\text{Ni}/\text{La} = 0.34$ for the sample heated above the dehydration temperature evidently shows that the losses of nickel from the film surface take place under heat treatment.

Comparison of O 1s spectra measurements *in situ* after annealing in super-high vacuum and after exposure to ambient for a short (~ 2 hours) time demonstrate a rapid water absorption and LNO surface hydroxidation. The resulting difference spectrum (Fig. 3, curve 6) is rather broad and may be deconvoluted into two components centred at about ~ 531 and ~ 533 eV due to $(\text{OH})^-$ and H_2O respectively. Finally, it may be concluded that even after surface cleaning and high temperature dehydration the intensity of the peak at ~ 531 eV remains comparable with the O^{2-} -anion peak intensity. This lateral peak may be attributed to low coordinated oxygen [13] and/or to oxygen-deficient regions [22] in the LNO matrix. Unfortunately, the

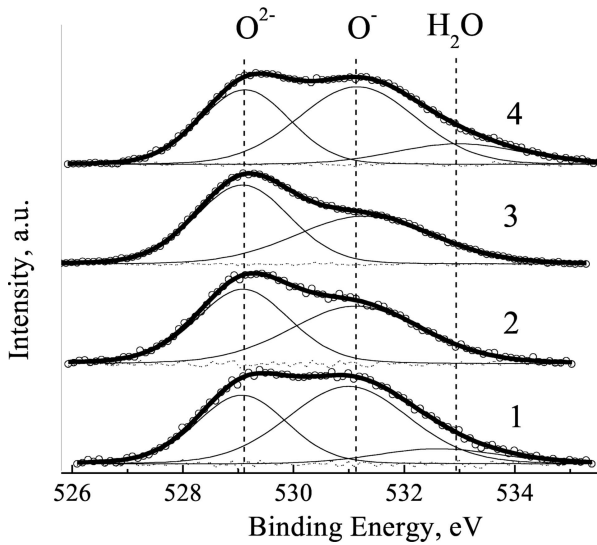


Fig. 5. Fitted O 1s spectra of highly-resistive dielectric LNO film V750: as-grown (1), after subsequent Ar^+ polishing (2), after subsequent super high vacuum annealing (550°C ; 30 h) (3), after subsequent exposure to ambient air for 2 hours (4). Symbols correspond to experimental data, the thick solid line to the spectra envelope, thin lines to spectral components, dotted lines to fitting residuals.

spectral resolution of the data is insufficient to allow the observation of more than two spectral components even for dehydrated films measured with good statistics. Our attempt to fit the spectrum with an individual component expected for O^- and $(\text{OH})^-$ species demonstrates that these various contributions cannot be fitted in an unambiguous way; consequently, they are represented by one broad peak.

This is also true for the high energy tail composed of peaks corresponding to various types of absorbed water species [17, 18]. That is the reason why we use the set of three peaks presenting the so-called O^{2-} , O^- (including hydroxyl group $(\text{OH})^-$), and H_2O species centred around 529, 531, and 533 eV respectively.

Several fitted spectra for dielectric LNO film before and after argon and temperature treatments (Fig. 5) demonstrate the effectiveness of such division for describing all spectra transformations due to film etching, annealing, and subsequent exposure to ambient atmosphere.

The same set of spectral components was used to fit a large number of spectra, recorded from different samples for further analysis of the effect of synthesis condition and subsequent annealing on the LNO films composition. For all treated samples, the energy separations (chemical shift) between the prime O^{2-} and lateral peaks are in surprisingly good agreement (Fig. 6), and slight variations in the lateral peak BE may be at-

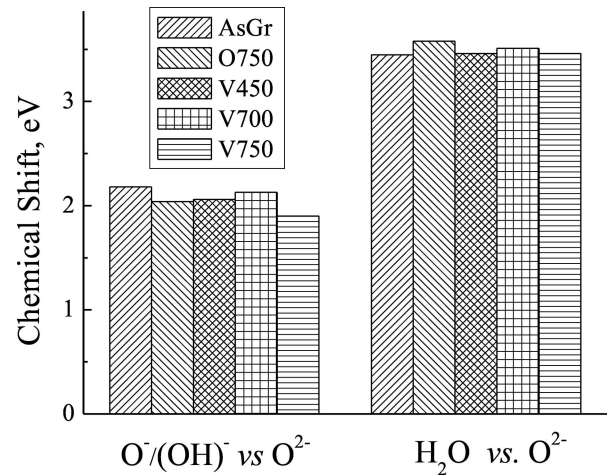


Fig. 6. Chemical shift of O 1s peaks corresponding to $\text{O}^-/(\text{OH})^-$ and H_2O species relatively the lattice oxygen O^{2-} peak for all treated films obtained by spectra fitting. Film annealing conditions are listed in Table 1.

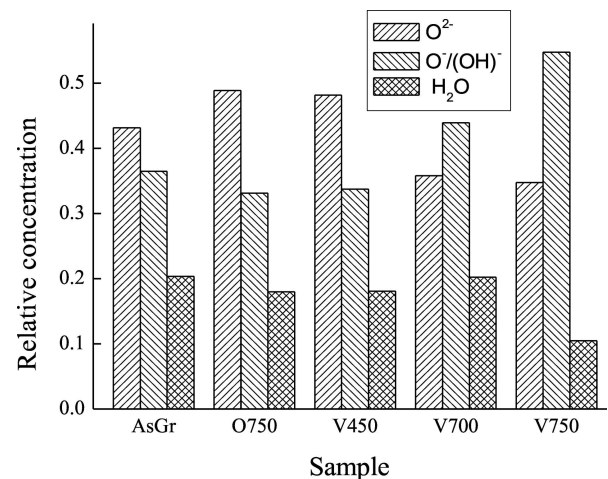


Fig. 7. Relative concentrations of various oxygen species for as-grown and annealed LNO films. Film annealing conditions are listed in Table 1.

tributed to the variation in the relative concentration of oxygen species contributing to peak broadening.

The effect of the thermal annealing on the relative concentration of various oxygen species concentration is shown in Fig. 7. It noteworthy that all films with dominating contribution of O^{2-} species (the O^{2-}/O^- concentration ratio $R_O > 1$) possess metallic type conductivity, while for films with $R_O < 1$ the temperature dependence of conductivity becomes semiconducting. Films remain metallic after high temperature ($\sim 750^\circ\text{C}$) annealing in oxygen atmosphere. This is also true for films annealed in vacuum at 450°C . However, significant changes in the oxygen species ratio R_O together with the accompanying conductivity conversion take place after high temperature annealing in vacuum. It is known that in $\text{LaNiO}_{3-\delta}$ transition

from metallic to insulating states takes place at $\delta = 0.25$ [23]. All this allows us to suppose that the loss of lattice O^{2-} ions during the vacuum annealing is responsible for this transformation.

The sharp increase in the O^- species concentration may be caused by the direct increase in the low coordinated oxygen content [14]. The increase in the number of oxygen vacancies, especially at the film surface, could be responsible for additional absorption of water, CO_2 , and O_2 molecules with a subsequent formation of lower charge oxygen ions. All of them may participate in the increase of the lateral peak intensity.

However, spectral resolution of the system is too low for unambiguous interpretation of XPS spectra, and relative concentrations of various oxygen species cannot be determined with appropriate accuracy. Further investigations are necessary for a detailed and quantitative understanding of the nature of the metal–insulator transformation after high temperature annealing.

4. Summary and conclusions

In summary, we studied the changes in the chemical composition and electrical conductivity of $LaNiO_{3-\delta}$ films under high temperature annealing. The technique used in the study was mainly O 1s X-ray photoelectron spectroscopy. The experimental spectrum of $LaNiO_{3-\delta}$ films was analysed in terms of O^{2-} , $O^-/(OH)^-$, and weakly adsorbed oxygen species. As-grown films deposited onto (100)-plane oriented $NdGdO_3$ substrate demonstrated excellent in-plane orientation and metallic behaviour. Films remained metallic and no significant changes in their resistance and O 1s XPS spectra were observed after annealing in oxygen at 10^5 Pa, $750^\circ C$. Conversion of the type of conductivity under high-temperature vacuum annealing may be attributed to the loss of lattice oxygen and reflects itself in the growth of the lateral peak at 531 eV in O 1s spectra. This increase in intensity may be attributed to the increasing number of oxygen vacancies with a subsequent increase in the concentration of low-coordinated oxygen species. These additional oxygen vacancies are likely to contribute greatly to rapid adsorption from ambient air and a significant increase in the surface contamination with O^- and $(OH)^-$ and weakly adsorbed oxygen species. The quantitative analysis of the La 3d_{3/2}-Ni 2p_{3/2} spectra region before and after the heat treatment shows the significant decrease of Ni/La concentration ratio. The losses of nickel species may be attributed to the nickel hydroxide decomposition after heating above the dehydration temperature.

These changes in the composition and electric properties of LNO films must be taken into account when the films are applied in optical and electrical devices.

References

- [1] J.B. Torrance, P. Lacorre, and A.I. Nazzari, Systematic study of insulator–metal transitions in perovskites $RNiO_3$ ($R = Pr, Nd, Sm, Eu$) due to closing of charge-transfer gap, *Phys. Rev. B* **45**, 8209–8212 (1992).
- [2] R. von Helmolt, J. Wecker, R. Holzapfel, L. Schultz, and K. Samwer, Giant negative magnetoresistance in perovskitelike $La_{2/3}Ba_{1/3}MnO_x$ ferromagnetic films, *Phys. Rev. Lett.* **71**, 2331–2333 (1993).
- [3] T. Venkatesan, M. Rajeswari, Z.-W. Dong, S.B. Ogale, and R. Ramesh, Manganite-based devices: opportunities, bottlenecks and challenges, *Philos. Trans. R. Soc. Lond. A* **356**, 1661–1680 (1998).
- [4] R. Ramesh, S. Aggarwal, and O. Auciello, Science and technology of ferroelectric films and heterostructures for non-volatile ferroelectric memories, *Mater. Sci. Eng. R Rep.* **32**, 191–236 (2001).
- [5] J. Choynet, N. Abadzhieva, P. Stefanov, D. Klissurski, J.M. Bassat, V. Rives, and L. Minchev, X-ray photoelectron spectroscopy, temperature-programmed desorption and temperature-programmed reduction study of $LaNiO_3$ and $La_2NiO_{4+\delta}$ catalysts for methanol oxidation, *J. Chem. Soc. Faraday Trans.* **90**, 1987–1993 (1994).
- [6] Y. Li, N. Chen, J. Zhou, S. Song, L. Liu, Z. Yin, and C. Cai, Effect of the oxygen concentration on the properties of Gd_2O_3 thin films, *J. Cryst. Growth* **265**, 548–552 (2004).
- [7] Q. Zhao, Z.M. Huang, Z.G. Hu, and J.H. Chu, A study on the thermostability of $LaNiO_3$ films, *Surf. Coatings Technol.* **192**, 336–340 (2005).
- [8] K. Horiba, R. Eguchi, M. Taguchi, A. Chainani, A. Kikkawa, Y. Senba, H. Ohashi, and S. Shin, *In situ* photoemission study of $LaNiO_3$ thin films grown by pulsed laser deposition, *J. Electron Spectros. Relat. Phenom.* **156**, 107–111 (2007).
- [9] V. Vengalis, A.K. Oginskas, V. Lissauskas, R. Butkutė, A. Maneikis, L. Dapkus, V. Jasutis, and N. Shiktorov, Growth and investigation of the $La_{1-x}Ca_xMnO_3/(LaNiO_3, RuO_2)$ heterostructures. In: *Thin Films Deposition of Oxide Multilayers. Industrial-Scale Processing*, Proceedings of International Conference, Vilnius, Lithuania, 28–29 September 2000, Vilnius, eds. A. Abrutis and B. Vengalis (University Press, Vilnius, 2000) pp. 45–48.
- [10] V. Bondarenka, S. Grebinskij, V. Lissauskas, S. Mickevičius, K. Šliuzienė, H. Tvardauskas, and B. Vengalis, XPS study of epitaxial $LaNiO_{3-x}$ films, *Lith. J. Phys.* **46**, 95–99 (2006).

- [11] S. Mickevičius, S. Grebinskij, V. Bondarenka, V. Lisauskas, K. Šliužienė, H. Tvardauskas, B. Vengalis, B.A. Orłowski, V. Osinniy, and W. Drube, The surface hydro-oxidation of LaNiO_{3-x} thin films, *Acta Phys. Pol. A* **112**, 113–120 (2007).
- [12] J. Haber, J. Stoch, and L. Ungier, X-ray photoelectron spectra of oxygen in oxides of Co, Ni, Fe and Zn, *J. Electron. Spectrosc. Relat. Phenom.* **9**, 459–467 (1976).
- [13] M.J. Tomellini, X-ray photoelectron spectra of defective nickel oxide, *J. Chem. Soc. Faraday Trans.* **84**, 3501–3511 (1988).
- [14] V.M. Jiménez, A. Fernández, J.P. Espinós, and A.R. González-Elipe, The state of the oxygen at the surface of polycrystalline cobalt oxide. *J. Electron. Spectrosc. Relat. Phenom.* **71**, 61–71 (1995).
- [15] T.J. Chuang, C.R. Brundle, and D.W. Rice, Interpretation of the x-ray photoemission spectra of cobalt oxides and cobalt oxide surfaces, *Surf. Sci.* **59**, 413–429 (1976).
- [16] H. Samata, D. Kimura, Y. Saeki, Y. Nagata, and T.C. Ozawa, Synthesis of lanthanum oxyhydroxide single crystals using anelectrochemical method, *J. Cryst. Growth* **304**, 448–451 (2007).
- [17] N.S. McIntyre and D.G. Zetaruk, X-ray photoelectron spectroscopy studies of iron oxides, *Anal. Chem.* **49**, 1521–1529 (1977).
- [18] A.R. Pratt, I.J. Muir, and H.W. Nesbitt, X-ray photoelectron and Auger electron spectroscopic studies of pyrrhotite and mechanism of air oxidation, *Geochim. Cosmochim. Acta* **58**, 827–841 (1994).
- [19] J.-C. Dupin, D. Gonbeau, P. Vinatier, and A. Levasseur, Systematic XPS studies of metal oxides, hydroxides and peroxides, *Phys. Chem. Chem. Phys.* **2**, 1319–1324 (2000).
- [20] V.G. Milt, C.A. Querini, and E.E. Miró, Thermal analysis of $\text{K}(x)/\text{La}_2\text{O}_3$, active catalysts for the abatement of diesel exhaust contaminants, *Thermochim. Acta* **404**, 177–186 (2003).
- [21] M. Sakashita and N. Sato, The structure and reactivity of nickel hydroxide, *Bull. Chem. Soc. Jpn.* **46**, 1983–1987 (1973).
- [22] J.H. Li, D.Z. Shen, J.Y. Zhang, D.X. Zhao, B.S. Li, Y.M. Lu, Y.C. Liu and X.W. Fan, Magnetism origin of Mn-doped ZnO nanoclusters, *J. Magn. Magn. Mater.* **302**, 118–121 (2006).
- [23] M. Abbate, G. Zampieri, F. Prado, A. Caneiro, J.M. Gonzalez-Calbet, and M. Vallet-Regi, Electronic structure and metal-insulator transition in $\text{LaNiO}_{3-\delta}$, *Phys. Rev. B* **65**, 155101 (2002).

EPITAKSINIŲ $\text{LaNiO}_{3-\delta}$ PLONŲ SKUOKSNIŲ PAVIRŠIAUS STABILUMAS

S. Mickevičius^a, S. Grebinskij^a, V. Bondarenka^{a,b}, H. Tvardauskas^a, M. Senulis^a, V. Lisauskas^a, K. Šliužienė^a, B. Vengalis^a, B.A. Orłowski^c, E. Baškys^a

^a *Fizinių ir technologijos mokslų centro Puslaidininkų fizikos institutas, Vilnius, Lietuva*

^b *Vilniaus pedagoginis universitetas, Vilnius, Lietuva*

^c *Lenkijos mokslų akademijos Fizikos institutas, Varšuva, Lenkija*

Santrauka

Plonieji daugiausia pseudokubine (100) kryptimi orientuoti $\text{LaNiO}_{3-\delta}$ sluoksniai gaminti reaktyvinio nuolatinės srovės magnetroninio dulkinimo būdu ir *in situ* atkaitinti O_2 ir vakuume. Sluoksnių sudėties kitimas kaitinimo metu tirtas Rentgeno fotoelektroninės spektroskopijos (RFS) metodu. Ištirti eksperimentiniai $\text{LaNiO}_{3-\delta}$ sluoksnių O 1s ir La 3d – Ni 2p_{3/2} spektrai, siekiant nustatyti O^{2-} , $\text{O}^-/(\text{OH})^-$ ir silpnai surišto deguonies santykius. Metalinio laidumo virtimą puslaidininkiniu atkaitinant va-

kuume aukštoje temperatūroje lydi žymus O 1s spektro 531 eV smailės intensyvumo padidėjimas. Šis intensyvumo augimas siejamas su deguonies vakansijų koncentracijos augimu ir lygiagrečiai su deguonies jonų su nutrauktais cheminiais ryšiais skaičiaus padidėjimu. Kiekybinė La 3d – Ni 2p_{3/2} spektro analizė rodo žymų Ni/La koncentracijų santykio sumažėjimą atkaitinus virš dehidracijos temperatūros. Toks laidumo ir paviršiaus sudėties kitimas aiškintinas deguonies netekimu gardelėje su vėlesne O^- ir $(\text{OH})^-$ anijonų bei silpnai surišto deguonies adsorbcija iš aplinkos oro.